Photoionization from the excited (3p, 3d, 4s, 4p) states of sodium

Anoop K Jain, S P Purohit* and K C Mathur

Department of Physics, University of Roorkee, Roorkee-247 667, India

Abstract : Calculations are presented for the total cross section (σ) and the angular distribution of asymmetry parameter (β) for photoionization from initial excited (3p, 3d, 4s and 4p) states of sodium atom. Comparison of our results for σ and β is made with other available theoretical calculations and the experimental data. We also present results for the angular distribution in electron-Na$^+$ elastic scattering at energies of $k = 0.5$ and $1.0\ a_0$.

Keywords : Photoionization, sodium atom, elastic scattering

PACS No. : 32.80.Fb

1. Introduction

Photoionization from the initial excited states of atoms has been a field of great interest in the last few decades both theoretically and experimentally. Photoionization of excited atoms represents one of the most fundamental collision processes. The study of such problems offers an opportunity to investigate the ionization processes from a given state of total energy and angular momentum. Recently, there has been a tremendous increase in the activity in this field mostly due to a great demand for such data on variety of atomic systems for their applications in many related areas such as controlled thermonuclear plasma, stellar atmosphere, fusion research and laser technology. More recently, it has been used in calculating the opacity [1–3] of stars under the international 'Opacity Project (OP)'. Furthermore, excited state photoionization is the inverse process to low-energy radiative recombination which is under current investigation [4].

Various theoretical studies on the photoionization from the excited states of atoms have been reported [5–22] in the literature. Manson and co-workers [16–18, 23,24] and

* Present address · Department of Physics, Kumaon Engineering College, Dwarahat, Almora-263 653, Uttar Pradesh, India

Saha and co-workers [12,13] have performed a series of calculations for the photoionization cross sections and photoelectron angular distribution asymmetry parameters in alkali-metal atoms. The experimental work on the photoionization from excited states is very little [19–22, 25–28]. In recent years, the availability of lasers as high intensity light sources and development of synchrotron radiation sources have advanced to such an extent that experimental work on metastable as well as non-metastable excited states of atoms is within the realm of possibility.

In this paper, we present a theoretical study of the photoionization from the initial excited states of sodium atom within the framework of non-relativistic central field approximation over a certain energy range above threshold. Results in the electric dipole approximation in velocity form are presented for the photoionization cross sections (σ) from the excited 3p, 3d, 4s and 4p states; and for the angular distribution asymmetry parameter (β) of the photoelectron produced by linearly polarized photons. Further, we also give results for the angular distribution in the electron-Na$^+$ elastic scattering in the static plus local exchange approximation. We have chosen sodium target for the present study with a view of possible future experimentation, since it is comparatively easier to prepare sodium atom target beams. Further, sodium being a low Z target, the spin orbit interaction and the relativistic effect would be small [29,30].

2. Theory

The total photoionization cross section, in the dipole approximation, from an initial (bound) state i to the final (continuum) state f is given by

$$\sigma(\omega) = 4\pi^2 \alpha a_0^2 \omega \sum_f \left| \left\langle \psi_f \left| T^d \right| \psi_i \right\rangle \right|^2, \qquad \bullet \qquad (1)$$

where T^d is the dipole transition operator which (in the velocity form) is given by

$$T^d = T_v^d = \sum_{j=1}^{N} \frac{\nabla_j}{i\omega}, \qquad (2)$$

where α is the fine structure constant and ω is the photon energy in atomic units. ψ_i and ψ_f are the initial and final atomic state wavefunctions respectively, which are taken to be antisymmetrized products of one electron wavefunctions. For the initial excited state we use the wavefunction of Kundu *et al* [31,32]. These are obtained from the frequency dependent calculations using the time dependent-coupled Hartree-Fock method. These wavefunctions can be expressed as,

$$\psi_i = P_{nl}(r) Y_{lm}(\hat{r}) \qquad (3)$$

where $$P_{nl}(r) = \sum_i C_i r^{n_i} \exp(-\Gamma_i r). \qquad (4)$$

$Y_{lm}(\hat{r})$ is the spherical harmonics and the radial function parameters C_i, n_i and Γ_i are defined by Kundu *et al* [31,32].

We have chosen these discrete state wavefunctions because TDCHF theory [33,34] furnishes accurate excitation energies and excited-state wavefunctions. The final state wavefunction is described in single-configuration $(1s^2\,2s^2\,2p^6, k)$ approximation, where the core orbitals $1s$, $2s$, $2p$ are taken from Clementi and Roetti [35] and the radial part of the continuum wavefunction is the solution of the radial Schrödinger equation in the static plus local exchange approximation.

The final state wavefunction for the ejected electron of momentum k is expressed as,

$$\psi_f = \frac{4\pi}{\sqrt{k}r} \sum_{lm} i^l \exp\big[i(\delta_l + \eta_l)\big] u_l(k,r) Y_{lm}(\hat{r}) Y^*_{lm}(\hat{k}), \tag{5}$$

where η_l and δ_l are the Coulomb and the non-Coulomb phase shifts respectively. The radial function u_l (k, r) is obtained by solving the following radial Schrödinger equation in the static plus local exchange approximation

$$\left[\frac{d^2}{dr^2} - \frac{l(l+1)}{r^2} - 2V(r) + k^2\right] u_l(k, r) = 0 \tag{6}$$

subject to the boundary conditions :

$$\lim_{r \to 0} u_l(k, r) = 0 \tag{7a}$$

and

$$\lim_{r \to \infty} u_l(k, r) = \frac{1}{\sqrt{k}}\big(\cos \eta_l F_l(k, r) + \sin \eta_l G_l(k, r)\big). \tag{7b}$$

F_l (k, r) and G_l (k, r) are the regular and irregular Coulomb wavefunctions respectively. The distorting potential $V(r)$ in eq. (6) is taken as

$$V(r) = V_{st}(r) + V_{ex}(r), \tag{8}$$

where $V_{st}(r)$ and $V_{ex}(r)$ are the static and exchange potentials respectively for electron-Na$^+$ scattering. The static potential $V_{st}(r)$ in e-Na$^+$ scattering is given by,

$$V_{st}(r) = -\frac{2}{r} + 2\left[\int_0^\infty R_{1s}^2 \frac{1}{r_>} r^2 dr + \int_0^\infty R_{2s}^2 \frac{1}{r_>} r^2 dr\right]$$

$$+ 6\left[\int_0^\infty R_{2p}^2 \frac{1}{r_>} r^2 dr + \frac{2}{5}\int_0^\infty R_{2p}^2 \frac{r_<^2}{r_>^3} r^2 dr\right], \tag{9}$$

where R_{nl}'s are the radial wavefunctions of Na$^+$ ion [35].

For evaluating the exchange potential $V_{ex}(r)$, we use the local approximation [36,37] and take,

$$V_{ex}(r) \simeq V_{ex}^{L}(r) = \frac{1}{2}\left[\left(\frac{1}{2}k^2 - V_{st}(r)\right) - \left(\left(\frac{1}{2}k^2 - V_{st}(r)\right)^2 + \alpha_d^2\right)^{1/2}\right], \quad (10)$$

where $\qquad \alpha_d^2 = 2\left(R_{1s}^2 + R_{2s}^2 + 3R_{2p}^2\right).$ $\qquad\qquad\qquad\qquad\qquad$ (11)

The differential cross section for the photoionization of an unpolarized target by the incident linearly polarized photons of energy ω is related to the angular distribution of photoelectrons in the electric dipole approximation by the following expression,

$$\frac{d\sigma_{nl}(\omega)}{d\Omega} = \frac{\sigma_{nl}(\omega)}{4\pi}\left[1 + \beta_{nl}(\omega)P_2(\cos\theta)\right], \quad (12)$$

where $\beta_{nl}(\omega)$ is the asymmetry parameter. P_2 is the Legendre polynomial and θ is the angle between the polarization vector $\hat{\varepsilon}$ of the incident photon and the direction $\hat{k}$ of the photoelectron momentum.

The total photoionization cross section $\sigma_{nl}(\omega)$, in the velocity form, for s, p and d states of the atom is obtained respectively as

$$\sigma_{ns}^{v}(\omega) = \frac{16\pi}{3}\alpha a_0^2 \frac{k}{(k^2 - \varepsilon_{ns})}d_{01}^2, \quad (13a)$$

$$\sigma_{np}^{v}(\omega) = \frac{16\pi}{9}\alpha a_0^2 \frac{k}{(k^2 - \varepsilon_{np})}\left(d_{10}^2 + 2d_{12}^2\right), \quad (13b)$$

$$\sigma_{nd}^{v}(\omega) = \frac{16\pi}{15}\alpha a_0^2 \frac{k}{(k^2 - \varepsilon_{nd})}\left(2d_{21}^2 + 3d_{23}^2\right) \quad (13c)$$

where the radial matrix elements d_{nl} are defined as

$$d_{01} = \frac{1}{\sqrt{k}}\int u_1(k,r)\frac{dP_{ns}(r)}{dr}r\,dr, \quad (14a)$$

$$d_{10} = \frac{1}{\sqrt{k}}\int u_0(k,r)\left(\frac{dP_{np}(r)}{dr} + 2\frac{P_{np}(r)}{r}\right)r\,dr, \quad (14b)$$

$$d_{12} = \frac{1}{\sqrt{k}}\int u_2(k,r)\left(\frac{dP_{np}(r)}{dr} - \frac{P_{np}(r)}{r}\right)r\,dr, \quad (14c)$$

$$d_{21} = \frac{1}{\sqrt{k}}\int u_1(k,r)\left(\frac{dP_{nd}(r)}{dr} + 3\frac{P_{nd}(r)}{r}\right)r\,dr, \quad (14d)$$

$$d_{23} = \frac{1}{\sqrt{k}}\int u_3(k,r)\left(\frac{dP_{nd}(r)}{dr} - 2\frac{P_{nd}(r)}{r}\right)r\,dr. \quad (14e)$$

The asymmetry parameter $\beta_{nl}(\omega)$ of the photoelectron angular distribution is given by [38],

$$\beta_{nl}(\omega) = \left[l(l-1)d_{l,l-1}^2(\omega) + (l+1)(l+2)d_{l,l+1}^2(\omega) \right.$$

$$\left. - 6l(l+1)d_{l,l-1}(\omega)d_{l,l+1}(\omega) \cos(\xi_{l+1} - \xi_{l-1}) \right] \Big/ (2l+1) \left[ld_{l,l-1}^2(\omega) \right.$$

$$\left. + (l+1)d_{l,l+1}^2(\omega) \right], \tag{15}$$

where $\xi_{l\pm1}(= \delta_{l\pm1} + \eta_{l\pm1})$ is the sum of the Coulomb and non-Coulomb phase shifts. In eq. (13), ε_{nl} are the orbital energies of sodium in Rydbergs.

In the present study, for obtaining σ and β we have preferred the use of velocity formulation, since the length form, which emphasizes regions of large r [39], will not be suitable for the excited state photoionization [16].

For the elastic scattering of electron with sodium ion (Na$^+$), the angular distribution is obtained from the following relation [40],

$$I(\theta) = \left(4k^4 \sin^4 \theta/2 \right)^{-1} + \left(k^3 \sin^2 \theta/2 \right)^{-1} \sum_l (2l+1)$$

$$* \cos\left[k^{-1} \ln(\sin^2 \theta/2) + 2(\delta_0 - \delta_l) - \eta_l \right] \sin \eta_l P_l(\cos \theta)$$

$$+ \left| k^{-1} \sum_l (2l+1) \exp\left[2i\delta_l + i\eta_l \right] \sin \eta_l P_l(\cos \theta) \right|^2. \tag{16}$$

The reduced differential cross section $R(\theta)$ is given by

$$R(\theta) = \frac{I(\theta)}{I_c(\theta)}, \tag{17}$$

where $I_c(\theta)$ is the differential cross section due to a pure Coulomb field and is given by

$$I_c(\theta) = \left[\frac{1}{2k^2 \sin^2(\theta/2)} \right]^2. \tag{18}$$

3. Results and discussion

The eqs. (1) to (15) have been used to obtain the total cross section (σ) and the asymmetry parameter (β) of the photoelectron angular distribution for the photoionization from the initial $3p$, $3d$, $4s$ and $4p$ excited states of sodium atom. The results thus obtained are shown in Figures 1–6. Further, we have also presented in Figure 7 the results of the angular distribution in electron-sodium ion elastic scattering.

Figure 1 shows the variation of the photoionization cross section (σ_{3p}) from the initial $3p$ excited state of Na as a function of the photoelectron energy in the energy range from threshold to 1.4 Ry. In the figure we compare our results with the other available
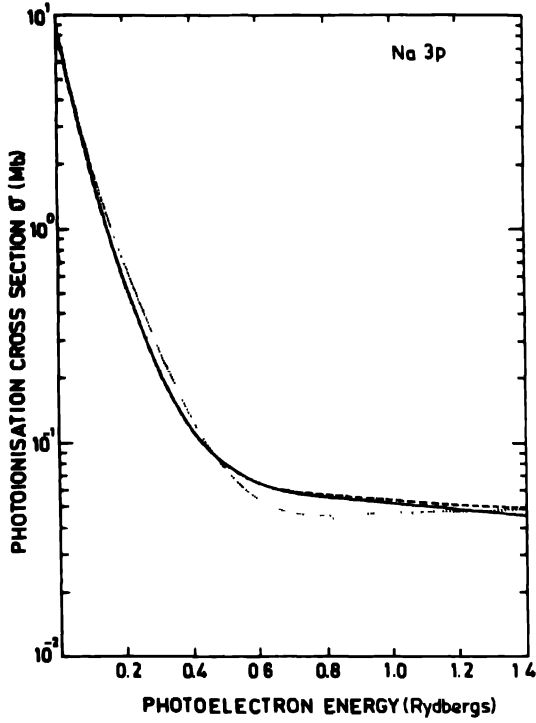
Figure 1. Total cross section for photoionization from the excited 3p state of Na.
———— present calculation, – – – – calculation of Preses *et al* [22] in the Hartree-Fock (HF) approximation; - - - - - calculation of Preses *et al* [22] in Hartree-Slater (HS) approximation.
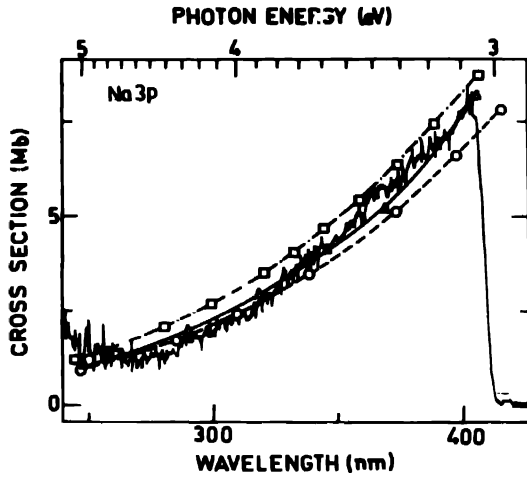

Figure 2. Total cross section for photoionization from the excited 3p state of sodium in the near threshold region.
–Δ– present results; —□—HS calculation [22]; – –O– – HF calculation [22]; ————experimental data of Preses *et al* [22].

calculations of Preses *et al* [22] using the Hartree-Fock (HF) and Hartreè-Slater (HS) wavefunctions. From the figure we notice that our results near threshold are in excellent agreement with both HF and HS calculations of Preses *et al*. In the higher energy region our results are in better agreement with the HF calculation than the HS calculation.

In Figure 2, we show a comparison of our results for σ_{3p} with the experimental data of Preses *et al* [22] from threshold to 2 eV above threshold. We find that our results of σ_{3p} agree very well with the experimental data also. From this figure, it is also seen that our theoretical calculations of σ_{3p} near threshold, lie approximately in between the central-field HF and HS cross section results of Preses *et al* [22].

In Figure 3, we present our calculation of the total photoionization cross section σ_{3d} from the excited 3d state of Na in the energy range of photoelectron energy from zero to 1.0 Ry. From these results, it is observed that the zeros which exist in the $3d \rightarrow k_p$ channels, have virtually no effect on the total photoionization cross section. This indicates the strong dominance of the $3d \rightarrow k_f$ channel on the total cross section. Comparison is made with the other available theoretical calculation of Msezane and Manson [16] which uses numerical Hartree-Fock wavefunctions. From the figure we find good agreement between two calculations.
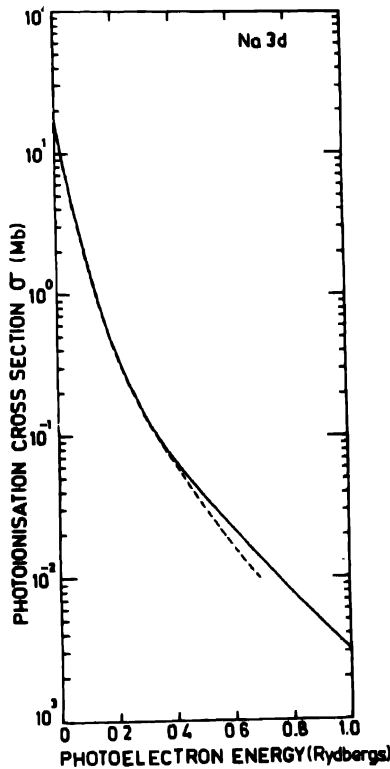

Figure 3. Total cross section for photoionization from the excited 3d state of Na
——— present calculation; – – – – calculation of Msezane and Manson [16] using numerical (NUM) initial state wavefunction.

In Figure 4, we plot the variation of the photoionization cross section σ_{4s} from the initial 4s excited state of Na as a function of the photoelectron energy in the energy range from zero to 0.5 Ry. Calculations of the photoionization cross sections have been performed using the TDCHF discrete wavefunction of Kundu and Mukherjee [31] and also the wavefunction of Daniele [41] obtained by effective potential approach (EPA). From the figure it is seen that from a threshold value of 3.2 Mb the TDCHF cross section (solid line) shows a deep minima at 0.12 Ry above threshold. The EPA cross section gives a threshold value of 0.87 Mb and decreases very rapidly to give a minima at about 0.05 Ry. Beyond the minima both the TDCHF and the EPA cross sections show an increase up to photoelectron energies of about 0.21 Ry and then decrease. The occurrence of minimum *i.e.* Cooper minima in the cross section arises due to the existence of zero in the dipole transition matrix element for the 4s $\rightarrow k_p$ channel. There is only $l \rightarrow l+1$ dipole matrix element in the case of s-state photoionization cross section. The TDCHF result shows a Cooper minima at a higher energy than the EPA results. Aymar *et al* [5] and D'yachkov and Pankratov [15] have also performed calculations for the photoionization cross sections of 4s state of sodium over a very small range of photoelectron energy above threshold. However, on comparison of the present threshold values of the cross sections with these calculations, it is found that their threshold values of cross sections lie in between the present threshold value of cross section obtained using the TDCHF wavefunction and the threshold value
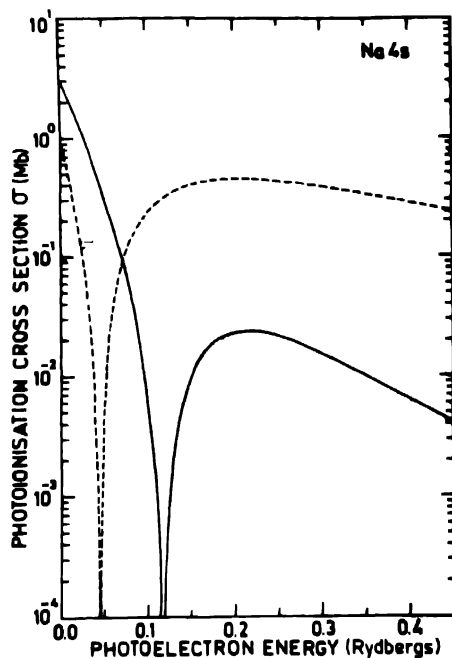

Figure 4. Total cross section for photoionization from the excited 4s state of Na.
——— present results using TDCHF wavefunction; – – – – present results using EPA wavefunction

obtained using the EPA wavefunction. At present, no experimental data for the photoionization from the excited $4s$ state of sodium is available to compare with the present calculations.

Figure 5 gives the plot of the total photoionization cross section σ_{4p} from the initial $4p$ excited state of Na in the photoelectron energy range from zero to 1 Ry. It is seen that for this transition, the photoionization cross section shows a smooth variation from its maximum value of 22.2 Mb at threshold to 0.025 Mb at energy of 1 Ry above threshold. We have also shown (in the inset) the cross section σ_{4p} against the wavelength where we compare our results with numerical quantum mechanical calculations of Aymar *et al* [5]. The semi classical analytical calculations of D'yachkov and Pankratov [15] gives the same results as that of Aymar *et al* over the entire region of wavelength. From this figure, it is seen that the present threshold cross section value of 22.2 Mb is within 20% of the corresponding value of 17.5 Mb obtained by Aymar *et al* [5] and D'yachkov and Pankratov [15], and 18.0 Mb (not shown in the figure) obtained by Burgess and Seaton [42] using the quantum defect method. The agreement between our calculation and that of Aymar *et al* [5] and D'yachkov and Pankratov [15] becomes better with the decrease in wavelength and by about 0.4 μm the two calculations agree completely.

Figure 6 shows our results for the asymmetry parameter β of the photoelectron angular distribution for Na ($3p$, $4p$ and $3d$) photoionization as a function of photoelectron energy from threshold to 1 Ry.
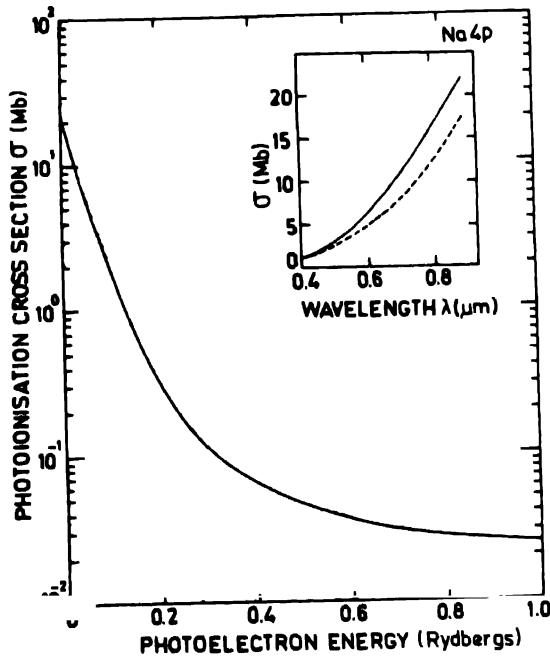

Figure 5. Total cross section for photoionization from the excited $4p$ state of sodium
———— present results; – – – – calculation of Aymar *et al* [5] using numerical quantum mechanical method.

In Figure 6(a), the asymmetry parameter β for the Na(3p) and Na(4p) photoionization are shown. From the expression of $\beta_{nl}(\omega)$ [in the eq. (15)], it is noticed that at the point where the matrix element corresponding to $p \rightarrow k_d$ channel becomes zero, the photoelectron angular distribution asymmetry parameter β would also be equal to zero. On the other hand, the value of β will be equal to 1 when the matrix element for $p \rightarrow k_s$ channel goes to zero. The asymmetry parameter $\beta_{nl}(\omega)$ depends on the accuracy of the dipole matrix amplitudes as well as the phase shifts. From the figure, it is seen that from a value of about 1.5 at threshold both β_{3p} (solid curve) and β_{4p} (broken curve) rise to a maximum value of about 2.0 at 0.15 Ry energy and then decreases. β_{3p} acquires a minimum value of about -0.5 at a photoelectron energy of 0.65 Ry beyond which it again shows an increase. Similarly, β_{4p} acquires a minimum value of about -0.4 at an energy of 0.8 Ry beyond which it again shows a slight increase. Looking at the figure, it is seen that β_{3p} passes through zero at two energies at about 0.47 Ry and 1.0 Ry above threshold. The Cooper minimum which is a consequence of zero in the $p \rightarrow k_d$ dipole matrix element lies at about 0.47 Ry and is therefore, responsible for the lower energy $\beta = 0$. The rapid variation in the asymmetry parameter β_{3p} as a function of photoelectron energy near the threshold region is mainly due

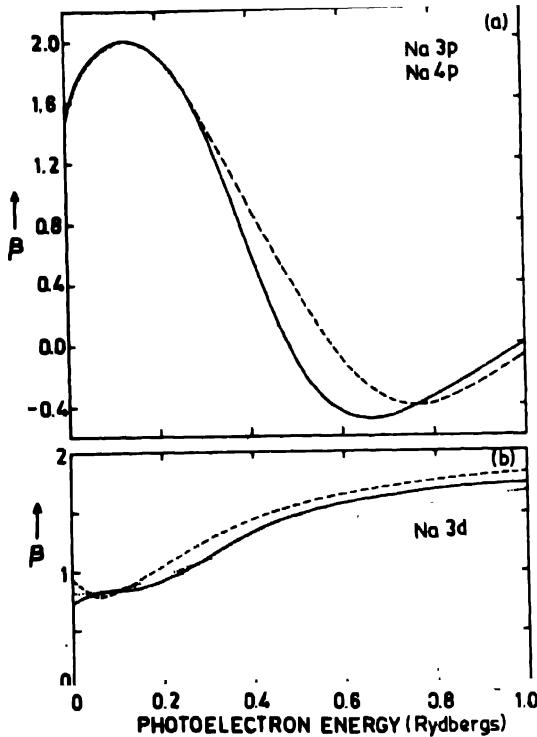Figure 6. Photoelectron angular distribution asymmetry parameter β of the excited 3p, 4p and 3d states of Na.

(a) ———— present results of Na(3p); — — — — present results of Na(4p). (b) ———— present results of Na(3d); — — — — calculation of Msezane and Manson [16] using analytic (PAR1) Hartree-Fock initial state wavefunction; . . . . . . calculation of Msezane and Manson [16] using numerical (NUM) initial state wavefunction.

to the strong interference between the $3p \rightarrow k_d$ and $3p \rightarrow k_s$ channels. The characteristic features of the results for β_{4p} are similar to the results for β_{3p}.

Figure 6(b) shows our results for the asymmetry parameter β for the Na(3d) photoionization. From the expression of $\beta_{nl}(\omega)$ [eq. (15)], it is seen that at the point where the dipole matrix element of $3d \rightarrow k_p$ channel is zero, the asymmetry parameter $\beta_{nl}(\omega)$ must be equal to 0.8. From this figure, it is seen that β_{3d} passes through 0.8 at 0.085 Ry which indicates the zero in $3d \rightarrow k_p$ channel. We compare our results with the calculations of Msezane and Manson [16] which uses the numerical (NUM) and analytic (PAR1) Hartree-Fock wavefunctions. We notice that our results are in reasonably good agreement with the calculations of Msezane and Manson and lie intermediate between their NUM and PAR1 results.

To our knowledge, no other theoretical calculations (or experimental measurements) of β for the Na (3p, 3d and 4p) photoionization is available for comparison with our results.

Figure 7 shows our results of the electron angular distribution in the elastic electron-sodium ion (Na$^+$) scattering at $k = 0.5\ a_0$ and $1.0\ a_0$ respectively in the range of scattering
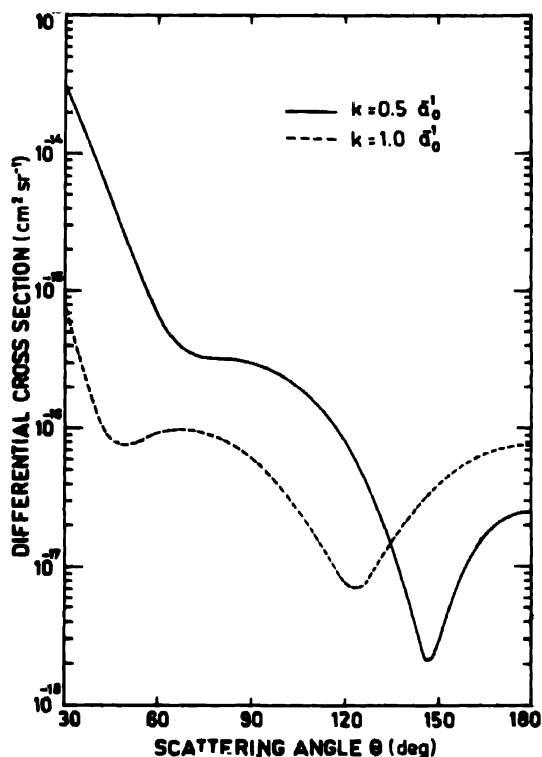

Figure 7. Differential cross section for the e-Na$^+$ elastic scattering.

present calculation at $k = 0.5\ a_0^{-1}$; – – – – present calculation at $k = 1\ a_0^{-1}$

Table 1. s-, p- and d-wave phase shifts in rad (relative to pure Coulomb phase shift) for elastic scattering of electrons from the Na$^+$ ion.

k (a.u.)	s-Wave phase shifts				p-Wave phase shifts				d-Wave phase shifts			
	Present results	DB1	DB2	DB3	Present results	DB1	DB2	DB3	Present results	DB1	DB2	DB3
0.1	4.165	4.151	4.227		2.608	2.624	2.687	2.691	0.026	0.019	0.051	0.059
0.2	4.159	4.146	4.221		2.597	2.613	2.676	2.680	0.029	0.021	0.054	0.057
0.3	4.148	4.137	4.212	4.205	2.580	2.597	2.659	2.666	0.034	0.026	0.062	0.065
0.4	4.133	4.126	4.198	4.192	2.557	2.575	2.637	2.643	0.041	0.032	0.072	0.074
0.5	4.115	4.111	4.181	4.177	2.529	2.548	2.609	2.615	0.050	0.040	0.084	0.084
0.6	4.094	4.093	4.161	4.158	2.497	2.517	2.577	2.583	0.061	0.051	0.099	0.096
0.7	4.069	4.071	4.138	4.136	2.462	2.483	2.543	2.548	0.074	0.063	0.117	0.110
0.8	4.042	4.047	4.112	4.111	2.426	2.447	2.506	2.511	0.089	0.079	0.137	0.125
0.9	4.012	4.020	4.083	4.083	2.388	2.410	2.468	2.473	0.105	0.096	0.159	0.142
1.0	3.980	3.991	4.052	4.053	2.350	2.372	2.430	2.434	0.123	0.116	0.183	0.161

Notation : DB1 – Exchange approx results of Dasgupta and Bhatia [43].

DB2 – Exchange adiabatic approx. results of Dasgupta and Bhatia [43].

DB3 – Polarized orbital approx results of Dasgupta and Bhatia [43].

Table 2. Reduced differential cross sections $R(\theta)$ for electron-Na$^+$ scattering

Angle θ (deg)	k = 0.3 a.u.		k = 0.4 a.u.		k = 0.5 a.u.		k = 0.6 a.u.	
	Present results	DB	Present results	DB	Present results	DB	present results	DB
10	0.989	0.993	1.027	1.029	0.980	0.987	0.965	0.965
20	1.070	1.072	0.898	0.903	1.036	1.011	1.167	1.143
30	0.845	0.855	1.132	1.092	1.298	1.282	1.190	1.213
40	1.082	1.040	1.369	1.361	1.142	1.189	0.824	0.896
50	1.386	1.366	1.132	1.179	1.708	0.777	0.416	0.476
60	1.225	1.250	0.710	0.764	0.382	0.419	0.260	0.265
70	0.863	0.899	0.458	0.483	0.336	0.331	0.394	0.358
80	0.638	0.659	0.448	0.451	0.494	0.478	0.672	0.645
90	0.589	0.602	0.551	0.559	0.676	0.689	0.892	0.921
100	0.592	0.611	0.611	0.646	0.735	0.797	0.918	1.016
110	0.546	0.579	0.558	0.620	0.628	0.727	0.728	0.870
120	0.441	0.490	0.413	0.491	0.410	0.517	0.419	0.553
130	0.325	0.389	0.250	0.329	0.183	0.270	0.137	0.221
140	0.252	0.332	0.138	0.214	0.042	0.096	0.0094	0.023
150	0.243	0.340	0.107	0.181	0.023	0.048	0.076	0.029
160	0.281	0.395	0.141	0.218	0.096	0.105	0.274	0.191
170	0.328	0.455	0.193	0.276	0.189	0.193	0.476	0.380
180	0.348	0.481	0.217	0.302	0.230	0.233	0.560	0.461

Notation · DB – Results of Dasgupta and Bhatia [43].

angles from 30° to 180° in the exchange approximation [36]. It is seen that for both the energies, the cross section shows a shoulder like structure in the angular region 60° to 90° at $k = 0.50\ a_0$ and 40° to 70° at $k = 1.0\ a_0$. Further at large scattering angles, a minimum in the cross sections is noticed at 147° scattering angle at 0.5 a_0 and at 123° scattering angle at 1.0 a_0 energy. Further, the phase shifts obtained by us at various electron energies in local exchange approximation, agree very well with those obtained by Dasgupta and Bhatia [43]. These phase shifts are listed in Table 1. Also in Table 2, we present our calculations for the reduced differential cross section $R(\theta)$. The reduced differential cross section is obtained as the ratio of the differential cross section $I(\theta)$ for the elastic scattering of electrons from the Na^+ ion to the differential cross section $I_c(\theta)$ due to a pure Coulomb field. As seen from this table our results agree very well with those obtained by Dasgupta and Bhatia [43] using exchange approximation.

From the comparison of experimental and theoretical data in above figures we conclude that the present calculations on sodium provide results which are in good agreement with the available data on photoionization cross sections and photoelectron distribution asymmetry parameters at photoelectron energies near the ionization threshold. These results show an emerging picture of the near threshold dynamics of the photoionization processes from the excited states of Na which suggest that the photoionization cross section is dominated by single particle processes. Experimentally, excited state photoionization cross sections have been measured over a limited energy range and the photoelectron angular distribution asymmetry parameter have been obtained for only a few single photon energies which are not sufficient to assess the accuracy of the theoretical models used for calculations. Finally we hope that the present calculations would provide impetus for further measurements on the photoionization cross sections and the photoelectron angular distribution asymmetry parameters from the excited states of sodium.

Acknowledgment

References

[1]   M J Seaton *J. Phys.* **B20** 6363 (1987)

[2]   P M J Sawey and K A Berrington *J. Phys.* **B25** 1451 (1992)

[3]   S N Nahar and A K Pradhan *J. Phys.* **B27** 429 (1994)   –

[4]   L H Andersen and J Bolko *J. Phys.* **B23** 3167 (1990)

[5]   M Aymar, E Luc-Koenig and F C Combet Farnoux *J. Phys.* **B9** 1279 (1976)

[6]   M Aymar *J. Phys.* **B11** 1413 (1978)

[7]   B Ritchie, M S Pindzola and W R Garrett *Phys. Rev.* **A23** 2905 (1981)

[8]   A Z Msezane and S T Manson *Phys. Rev. Lett.* **35** 364 (1982)

[9]   N B Avdonina and M Ya Amusia *J. Phys.* **B16** L543 (1983)

[10] A Z Msezane *Phys. Rev.* **A29** 3431 (1984)

[11] C E Burkhardt, J L Libbert, Xu Jian, J J Leventhal and J D Kelley *Phys. Rev.* **A38** 5949 (1988)

[12] H P Saha, M S Pindzola and R N Compton *Phys. Rev.* **A38** 128 (1988)

[13] H P Saha *Phys. Rev.* **A41** 174 (1990)

[14] D Cubayanes, J M Bizau, F J Wuilleumier, B Carre and F Gounand *Phys. Rev. Lett.* **63** 2460 (1989)

[15] L G D'yachkov and P M Pankratov *J. Phys.* **B27** 461 (1994)

[16] A Z Msezane and S T Manson *Phys. Rev.* **A30** 1795 (1984)

[17] A Z Msezane, J Lahiri and S T Manson *Phys. Rev.* **A33** 4406 (1986)

[18] S N Nahar and S T Manson *Phys. Rev* **A40** 6300 (1989)

[19] A V Smith, J E M Goldsmith, D E Nitz and S J Smith *Phys Rev.* **A22** 577 (1980)

[20] K Gerwert and K J Kollath *J. Phys.* **B16** L217 (1983)

[21] S L Gilbert, M C Noecker and C E Wieman *Phys. Rev.* **A29** 3150 (1984)

[22] J M Preses, C E Burkhardt, R L Corey, D L Earsom, T L Daulton, W P Garver, J J Leventhal, A Z Msezane and S T Manson *Phys Rev.* **A32** 1264 (1985)

[23] J Lahiri and S T Manson *Phys Rev. Lett* **48** 614 (1982)

[24] J Lahiri and S T Manson *Phys. Rev.* **A33** 3151 (1982)

[25] H T Duong, J Pinard and J L Vialle *J. Phys.* **B11** 797 (1978)

[26] J C Hansen, A J Duncanson (Jr.), R L Chien and R S Berry *Phys Rev.* **A21** 222 (1980)

[27] L E Cuellar, R N Compton, H S Carman (Jr) and C S Feigerle *Phys Rev Lett.* **65** 163 (1990)

[28] D J Armstrong, L A Westling and S J Smith *Phys. Rev.* **A43** 6398 (1991)

[29] J C Weisheit *Phys Rev.* **A5** 1621 (1972)

[30] J J Chang and H P Kelly *Phys. Rev.* **A5** 1713 (1972)

[31] B Kundu and P K Mukherjee *Phys Rev.* **A35** 980 (1987)

[32] B Kundu, D Ray and P K Mukherjee *Phys. Rev.* **A34** 62 (1986)

[33] C W McCurdy, T Rescigno, D L Yeager and V McKoy *Methods of Atomic Structure Theory* (New York : Plenum) **Vol. III** p 339 (1877)

[34] J Oddershede *Adv Quantum Chem.* **11** 257 (1978)

[35] E Clementi and C Roetti *At. Data Nucl. Data Tables* **14** (1974)

[36] J B Furness and I E McCarthy *J. Phys.* **B6** 2280 (1973)

[37] M E Riley and D G Truhlar *J. Chem. Phys.* **63** 2182 (1981)

[38] J Cooper and R N Zare *Lectures in Theoretical Physics* (New York : Gordon and Breach) **Vol. XI-C** (1969)

[39] L M Branscomb *Atomic and Molecular Processes* (New York : Academic) p 104 (1962)

[40] L Schiff *Quantum Mechanics* (New York : McGraw-Hill) p 116 (1955)

[41] R Daniele *J. Chem. Phys.* **72** 1276 (1980)

[42] A Burgess and M J Seaton *Mon. Not. Roy. Astron. Soc.* **120** 121 (1960)

[43] A Dasgupta and A K Bhatia *Phys. Rev.* **A31** 759 (1985)